



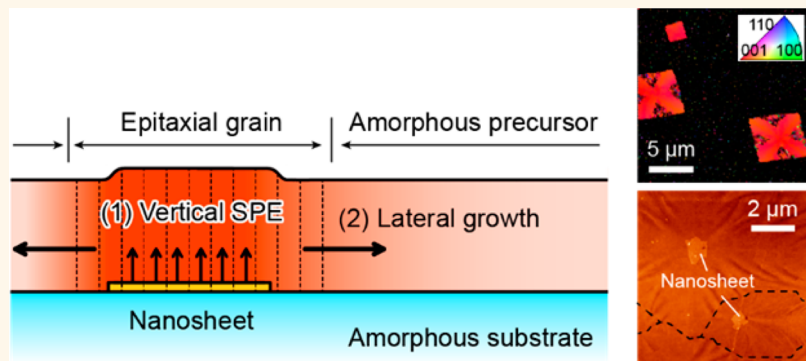
Lateral Solid-Phase Epitaxy of Oxide Thin Films on Glass Substrate Seeded with Oxide Nanosheets

Kenji Taira,[†] Yasushi Hirose,^{†,‡,§,*} Shoichiro Nakao,^{‡,§} Naomi Yamada,^{‡,§} Toshihiro Kogure,^{§,||} Tatsuo Shibata,^{§,⊥} Takayoshi Sasaki,^{§,⊥} and Tetsuya Hasegawa^{†,‡,§}

[†]Department of Chemistry, Graduate School of Science, The University of Tokyo, 7-3-1 Hongo, Bunkyo-ku, Tokyo 113-0033, Japan, [‡]Kanagawa Academy of Science and Technology, 3-2-1 Sakado, Takatsu-ku, Kawasaki 213-0012, Japan, [§]CREST, Japan Science and Technology Agency, 4-1-8 Honcho, Kawaguchi 332-0012, Japan,

^{||}Department of Earth and Planetary Science, Graduate School of Science, The University of Tokyo, 7-3-1 Hongo, Bunkyo-ku, Tokyo 113-0033, Japan, and [⊥]National Institute for Materials Science, 1-1 Namiki, Tsukuba 305-0044, Japan

ABSTRACT



We developed a technique to fabricate oxide thin films with uniaxially controlled crystallographic orientation and lateral size of more than micrometers on amorphous substrates. This technique is lateral solid-phase epitaxy, where epitaxial crystallization of amorphous precursor is seeded with ultrathin oxide nanosheets sparsely ($\approx 10\%$ coverage) deposited on the substrate. Transparent conducting Nb-doped anatase TiO_2 thin films were fabricated on glass substrates by this technique. Perfect (001) orientation and large grains with lateral sizes up to $10 \mu\text{m}$ were confirmed by X-ray diffraction, atomic force microscopy, and electron beam backscattering diffraction measurements. As a consequence of these features, the obtained film exhibited excellent electrical transport properties comparable to those of epitaxial thin films on single-crystalline substrates. This technique is a versatile method for fabricating high-quality oxide thin films other than anatase TiO_2 and would increase the possible applications of oxide-based thin film devices.

KEYWORDS: oxide nanosheets · lateral solid-phase epitaxy · thin film · transparent conducting electrode · TiO_2 · perovskite

The physical properties of a crystalline thin film generally depend on its crystallographic features, especially on its crystallographic orientation and grain size. To control these features, the underlying substrate plays a crucial role. For example, epitaxial thin films grown on lattice-matched single-crystalline substrates can exhibit specific structures and orientations with less or no grain boundaries. In contrast, films fabricated on amorphous substrates such as glass or plastic, which are of industrial importance owing to their low cost and large size availability, usually take polycrystalline form with random orientation and

high densities of grain boundaries. As a consequence, polycrystalline films on amorphous substrates tend to possess degraded properties, represented by low electric conductivity due to electron scattering at the grain boundaries, in comparison with those of single-crystalline films.

Several techniques have thus far been developed for controlling crystallographic orientation on amorphous or polycrystalline substrates, including ion-beam-assisted deposition and inclined substrate deposition methods.^{1,2} However, in most of these techniques, it is difficult to enlarge grain size above sub-micrometer scale because of

* Address correspondence to hirose@chem.s.u-tokyo.ac.jp.

Received for review March 20, 2014 and accepted May 22, 2014.

Published online May 27, 2014
10.1021/nn501563j

© 2014 American Chemical Society

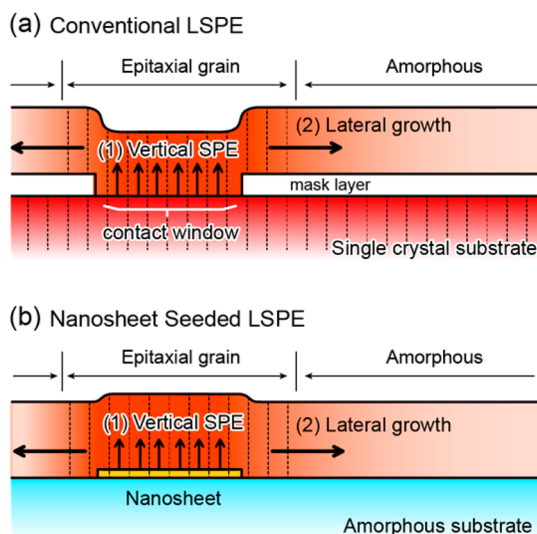


Figure 1. Schematic illustration of (a) conventional LSPE on single-crystal substrate and (b) NS-LSPE on glass substrate.

uncontrollable nucleation on the substrate, especially if the films are very thin. Recently, another approach using “oxide nanosheets” has been proposed for uniaxial orientation control of oxide thin films such as perovskite oxides, anatase TiO_2 , and ZnO .^{3–7} Oxide nanosheets are ultrathin (≈ 1 nm thick) sheet-like oxide single crystals prepared by soft chemical processes,⁸ and amorphous substrates densely covered with oxide nanosheets have been used as templates for epitaxial growth of materials. The obtained epitaxial thin films were confirmed to show improved properties, such as enhanced conductivity in transparent conducting $\text{Nb}:\text{TiO}_2$ thin films reported by Yamada *et al.*,⁹ high dielectric constant in $\text{Ba}_{0.5}\text{Sr}_{0.5}\text{TiO}_3$ thin films by Jung *et al.*,¹⁰ and increased electric polarization in ferroelectric $\text{Pb}(\text{Zr},\text{Ti})\text{O}_3$ (ref 6) and $\text{SrBi}_4\text{Ti}_4\text{O}_{15}$ (ref 11) thin films by Kikuta *et al.* and Kondoh *et al.*, respectively. However, even in the above-mentioned oxide nanosheet seed layer technique, the lateral sizes of the crystal grains were limited by those of the nanosheets, typically less than several micrometers, and the influence of the grain boundaries on film properties was still not negligible.

To overcome the limitation of lateral grain size, we combined the nanosheet seed layer technique with solid-phase crystallization of an amorphous precursor thin film, which is effective for increasing lateral grain size in a variety of thin film materials such as Si,¹² $\text{In}_{2-x}\text{Ga}_x\text{O}_3$,^{13,14} and TiO_2 .¹⁵ Conceptually, this technique is a kind of lateral solid-phase epitaxy (LSPE), which was originally developed for fabricating silicon-on-insulator structures.¹⁶ In conventional LSPE of Si, single-crystalline Si substrates masked by a SiO_2 layer containing small contact windows work as seeds for epitaxial crystallization of amorphous Si deposited on the substrates (Figure 1a). In contrast, in our technique, hereafter referred to as nanosheet-seeded LSPE

(NS-LSPE), an amorphous substrate is sparsely covered with lattice-matched oxide nanosheets, which play an analogous role in the contact windows in the conventional LSPE (Figure 1b). An amorphous precursor film is deposited on this substrate and subsequently crystallized by postdeposition annealing. At the beginning of the crystallization process, vertical solid-phase epitaxy (VSPE) with the nanosheet seeds provides epitaxial nuclei, and these nuclei successively grow in the lateral direction beyond the edges of the nanosheets. The grains continue to grow until they come into contact with neighboring grains and thus cover the whole film region.

In this study, we demonstrate the NS-LSPE technique by fabricating highly conductive (001)-oriented $\text{Nb}:\text{TiO}_2$ thin films with large lateral grain sizes. Anatase TiO_2 is suitable for a prototypical study of NS-LSPE because epitaxial growth of anatase TiO_2 on $\text{Ca}_2\text{Nb}_3\text{O}_{10}$ nanosheets has been reported using various film deposition processes, such as sol–gel,³ pulsed laser deposition (PLD),⁴ and sputtering.⁹ Furthermore, $\text{Nb}:\text{TiO}_2$ is a promising indium-free transparent oxide conductor,¹⁷ and controlling crystallographic orientation of individual grains^{9,18} and enlarging lateral grain sizes¹⁹ are key to further improving its electric conductivity.

RESULTS AND DISCUSSION

A $\text{Nb}:\text{TiO}_2$ thin film was fabricated at the outset by a conventional solid-phase crystallization process²⁰ on a alkaline-free glass substrate sparsely covered with $\text{Ca}_2\text{Nb}_3\text{O}_{10}$ nanosheets ($\approx 10\%$ coverage ratio): an ≈ 80 nm thick amorphous $\text{Nb}:\text{TiO}_2$ precursor film was deposited on the substrate without intentional substrate heating and successively crystallized by annealing under H_2 atmosphere. Contrary to our expectation, the θ – 2θ X-ray diffraction (XRD) profile of the crystallized film revealed an intense 101 diffraction peak of the anatase structure, and the 004 peak, which should be dominant in c-axis oriented films, was very weak (Figure 2a). Moreover, these diffractions were recorded as Debye ring patterns in the two-dimensional detector image. These XRD results clearly indicate that, under these conditions, even with a nanosheet seed, a randomly oriented polycrystalline film was obtained (Figure 2c, top).

The introduction of an epitaxial anatase TiO_2 as “secondary seed” layer is known to be effective in achieving vertical epitaxial growth of (001)-oriented anatase TiO_2 on perovskite substrate.^{21,22} Prior to the deposition of amorphous precursor films, we grew thin $\text{Nb}:\text{TiO}_2$ secondary seed layers with various thicknesses (1, 3, and 5 nm) on the substrates at $T_s = 400$ °C, which is high enough for epitaxial growth of anatase TiO_2 on the $\text{Ca}_2\text{Nb}_3\text{O}_{10}$ nanosheets.⁴ After the samples were cooled at room temperature, ≈ 80 nm thick amorphous $\text{Nb}:\text{TiO}_2$ films were deposited on the secondary seed

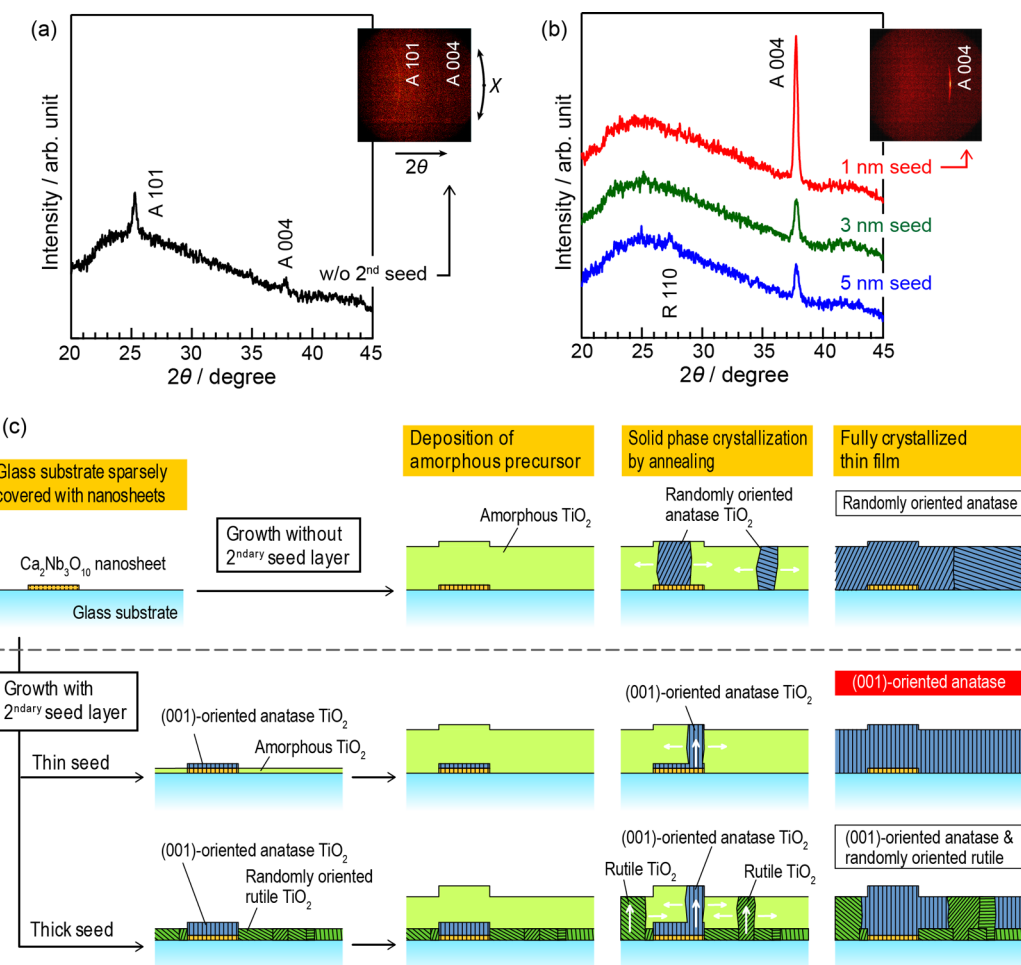


Figure 2. (a,b) XRD patterns of Nb:TiO₂ thin films crystallized on glass substrate sparsely covered with Ca₂Nb₃O₁₀ nanosheets; (a) θ - 2θ profile of the Nb:TiO₂ film without secondary seed layer and (b) those with secondary seed layers. Labels “A” and “R” represent diffraction from anatase and rutile TiO₂, respectively. Two-dimensional area detector images are also shown. (c) Schematic illustrations of Nb:TiO₂ thin films crystallized on glass substrate sparsely covered with Ca₂Nb₃O₁₀ nanosheets; (top) Nb:TiO₂ film grown without secondary seed layer, (middle) Nb:TiO₂ film grown with thin secondary seed layer, and (bottom) Nb:TiO₂ film grown with thick secondary seed layer.

layer and crystallized by the same procedure as that mentioned above. Figure 2b shows the θ - 2θ XRD profiles of the Nb:TiO₂ thin films crystallized on the secondary seed layers of various thicknesses. As seen from the figure, the insertion of the secondary seed layer drastically improved the crystallographic orientation. In particular, the XRD profile of the Nb:TiO₂ film fabricated on 1 nm thick secondary seed layer exhibited only the 004 diffraction of anatase structure, proving the solid-phase epitaxial growth of (001)-oriented anatase Nb:TiO₂. The tight-arc-shaped diffraction on the two-dimensional detector image also validates the (001)-oriented growth of anatase Nb:TiO₂. In contrast, the Nb:TiO₂ films on thicker secondary seed layers (3 and 5 nm) showed weakened 004 diffraction of anatase together with 110 diffraction from randomly oriented rutile crystals, which is thermodynamically more stable. This can be rationalized by assuming that the thicker secondary seed layer (3 or 5 nm) deposited on bare glass regions crystallized into

polycrystalline rutile phase, which further assisted the crystallization of rutile Nb:TiO₂ film on it (Figure 2c, bottom). Conversely, the ultrathin (1 nm) secondary seed layer on bare glass is perhaps in the amorphous phase and did not act as nucleation centers (Figure 2c, middle). Mitchel *et al.*²³ investigated atomic layer deposition of TiO₂ films on amorphous substrates and found that the substrate temperature at which the crystallization occurs increased with decreasing film thickness. Consequently, they suggested that the crystallization of TiO₂ is triggered by stress in the film accumulated during film deposition. This crystallization mechanism can account for the XRD results in Figure 2b: a thicker secondary seed layer on glass crystallized into rutile owing to sufficient accumulation of stress, and the produced fine rutile crystals behaved as randomly oriented seeds for the crystallization of amorphous Nb:TiO₂ film.

Hereafter, we focused on Nb:TiO₂ thin films fabricated on 1 nm thick secondary seed layer. First, in order

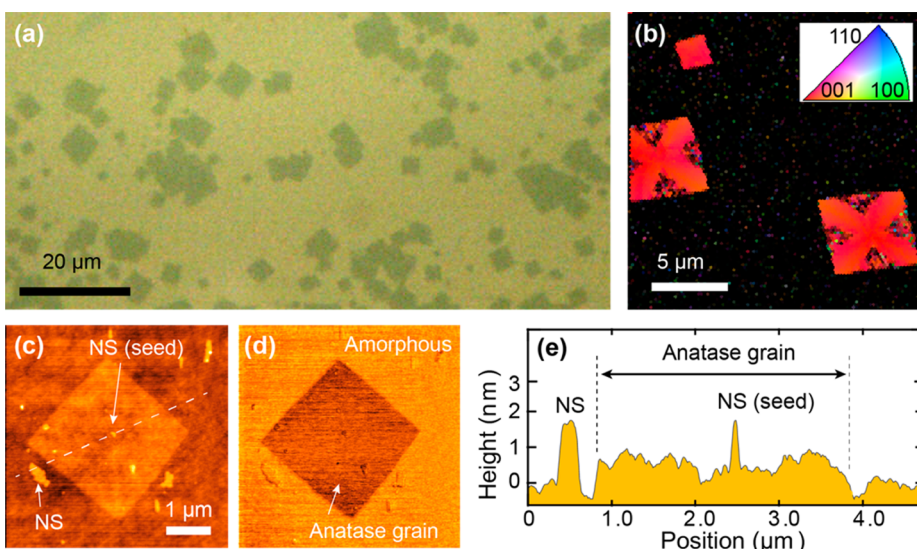


Figure 3. (a) Optical microscope image of a partially crystallized Nb:TiO₂ thin film fabricated by NS-LSPE with 1 nm thick secondary seed layer. (b) Inversed pole figure map of the same sample colored with the crystallographic orientation along the normal direction. Black areas represent amorphous regions. (c) AFM and (d) FFM images of the region around a (001)-oriented anatase grain. Both the images were obtained simultaneously. (e) Line profile of surface morphology along the dashed line in (c). Positions of the nanosheets in (c) and (e) are labeled by “NS”.

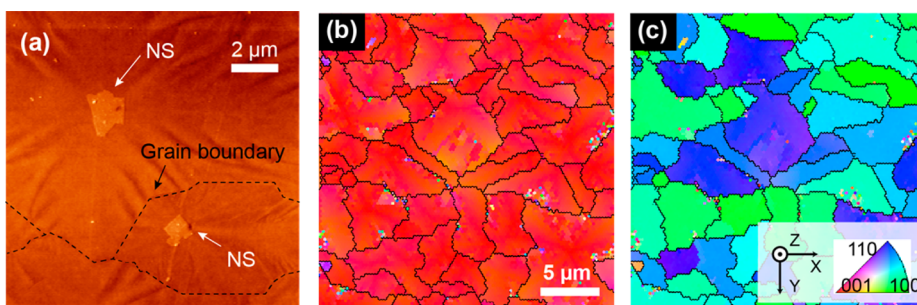


Figure 4. (a) AFM image of a fully crystallized Nb:TiO₂ thin film fabricated by NS-LSPE with 1 nm thick secondary seed layer. Dashed lines indicate grain boundaries. Positions of the nanosheets are labeled by “NS”. (b,c) Inversed pole figure maps of the fully crystallized Nb:TiO₂ film. Crystallographic orientation along the surface normal (Z) and the transverse (X) direction was mapped in (b) and (c), respectively. The solid lines in (b) and (c) indicate grain boundaries.

to verify the lateral growth of Nb:TiO₂ starting from nanosheets as crystallization nuclei, we prepared partially crystallized Nb:TiO₂ thin films by quenching them during postdeposition annealing. An optical microscope image (Figure 3a) of the partially crystallized film revealed evolution of square-shaped grains in amorphous precursor matrix. These grains were assigned to (001)-oriented anatase Nb:TiO₂ crystals by electron backscattering diffraction (EBSD) measurements (Figure 3b), consistent with the XRD results. Figure 3c is an atomic force microscopy (AFM) image around a (001)-oriented anatase Nb:TiO₂ grain. The anatase Nb:TiO₂ grain located at the center of the image is ≈1.0 nm higher than the surrounding amorphous matrix, reflecting volume expansion accompanied by crystallization, which is more clearly visualized in the friction force microscopy (FFM) image (Figure 3d). Notably, the AFM image in Figure 3c also resolves a tiny piece of single-layer Ca₂Nb₃O₁₀ nanosheet with a height of ≈1.5 nm (Figure 3e) at the center

of the square Nb:TiO₂ grain. This proves that the (001)-oriented anatase grain grew in the lateral direction from the primary seeding nanosheet. The lateral sizes of the fully crystallized anatase Nb:TiO₂ grains determined from AFM (Figure 4a) and EBSD (Figure 4b,c) measurements were in the range of ≈3–10 μm, which is much larger than those of the Ca₂Nb₃O₁₀ nanosheets used in this study (<≈2 μm). It seems that the lateral growth of anatase grains came to an end when adjacent grains encountered each other (Figure 4a), suggesting the possibility that the grains may be further enlarged by optimizing the average distance between nanosheets.

Finally, we examined the electrical transport properties of the (001)-oriented Nb:TiO₂ film fabricated by NS-LSPE. Table 1 summarizes the resistivity ρ , carrier density n , and Hall mobility μ of the anatase Nb:TiO₂ thin films grown by various methods. The ρ value of the film fabricated by NS-LSPE, $3.6 \times 10^{-4} \Omega \text{ cm}$, is the lowest ever reported for Nb:TiO₂ thin film on glass

TABLE 1. Electrical Transport Properties of Anatase $\text{Nb}_{0.06}\text{Ti}_{0.94}\text{O}_2$ Thin Films Fabricated by Various Techniques

fabrication technique	crystallographic orientation	ρ ($\Omega \text{ cm}$)	n (cm^{-3})	μ ($\text{cm}^2 \text{ V}^{-1} \text{ s}^{-1}$)	ref
PLD, NS-LSPE on glass	(001)	3.6×10^{-4}	1.3×10^{21}	13	this work
PLD, solid-phase crystallization on glass	random	5.6×10^{-4}	1.4×10^{21}	8.0	20
RF sputtering, nanosheet seed layer on glass	(001)	4.0×10^{-4}	1.7×10^{21}	9.1	9
PLD, epitaxial growth on $(\text{LaAlO}_3)_{0.3}(\text{SrAl}_0.5\text{Ta}_{0.5}\text{O}_3)_{0.7}$ (100)	(001)	2.3×10^{-4}	1.7×10^{21}	16	17

substrate, which is obviously a consequence of its very high μ ($13 \text{ cm}^2 \text{ V}^{-1} \text{ s}^{-1}$) comparable to that of epitaxial thin film on single-crystalline substrate ($16 \text{ cm}^2 \text{ V}^{-1} \text{ s}^{-1}$). This μ value is not only $\approx 60\%$ higher than that of randomly oriented polycrystalline films obtained by conventional solid-phase crystallization but also $\approx 40\%$ higher than that of (001)-oriented films fabricated on densely deposited nanosheet seeds.⁹ Such substantial improvement in μ is attributable to the enlargement of grains, that is, less density of grain boundaries, as well as the reduction of effective electron mass by (001) orientation.^{9,18}

CONCLUSIONS

In conclusion, we have developed the NS-LSPE technique and fabricated Nb:TiO₂ thin films with

uniaxially controlled crystallographic orientation and large lateral grain size on amorphous substrates. As a consequence of its well-controlled crystallographic orientation and enlarged grains with lateral sizes up to $10 \mu\text{m}$, the Nb:TiO₂ thin film obtained by the NS-LSPE exhibited excellent transport properties comparable to those of epitaxial thin films on lattice-matched single-crystalline substrates. The NS-LSPE technique is expected to be a versatile method for fabricating high-quality oxide thin films other than anatase TiO₂ on amorphous substrate and will increase the applications of oxide-based thin film devices. Indeed, we have achieved orientation control of a perovskite oxide, SrTiO₃, which is a key material in oxide-based electronics (Figure S1, Supporting Information).

MATERIALS AND METHODS

Preparation of Substrates. Ca₂Nb₃O₁₀ nanosheets (2D perovskite, $a = 0.386 \text{ nm}$, ref 5) were used as templates for (001)-oriented anatase Nb:TiO₂ ($a = 0.379 \text{ nm}$). The preparation of the colloidal suspension of the nanosheets was described elsewhere.³ The size of nanosheets has large dispersion from less than 100 nm to $\approx 2 \mu\text{m}$. The Ca₂Nb₃O₁₀ nanosheets were sparsely deposited on alkaline-free glass substrates (Corning EAGLE2000) by immersing the substrates into the colloidal suspension for several seconds. After the immersion, residual water droplets were blown off with N₂ gas. The coverage ratio of the Ca₂Nb₃O₁₀ nanosheets was evaluated to be $< 10\%$ from AFM images.

Fabrication of Thin Films. Amorphous Nb:TiO₂ precursor films were fabricated on the unheated substrates by PLD. A KrF excimer laser (248 nm, 1 J cm^{-2} pulse⁻¹, 2 Hz) was used to ablate a sintered pellet of Nb_{0.06}Ti_{0.94}O₂. The partial oxygen gas pressure (P_{O_2}) was set at 10^{-3} Torr during the deposition. The typical thickness of the films measured with a stylus profiler was $\approx 80 \text{ nm}$ after 2 h deposition. The anatase Nb:TiO₂ secondary seed layers were also fabricated by PLD at $T_s = 400^\circ\text{C}$. The thickness of the secondary seed layers were estimated from the deposition time. The precursor films were crystallized by post-deposition annealing at 600°C for 1 h under H₂ atmosphere (1 atm) in an infrared image furnace (Ulvac, MILA-3000PN). Partially crystallized films were prepared by interrupting the annealing and quenching the film to room temperature when the resistance of the film started decreasing, a signature of crystallization.²⁰

Thin Film Characterization. The crystallographic structure and orientation of the films were determined using an X-ray (Cu K α) diffractometer with a two-dimensional area detector (Bruker, discover d8 with GADDS) and an EBSD mapping system equipped on a field emission scanning electron microscope (JEOL, JSM7000F). The microstructure of the films was characterized with an optical microscope and a scanning probe microscope (SII-nanotechnology, SPI4000 with SPA400). The electrical transport properties of the crystallized film were evaluated at room temperature using four-probe resistance and Hall measurements with standard six-probe configuration.

Conflict of Interest: The authors declare no competing financial interest.

Acknowledgment. Part of this work was conducted in the Research Hub for Advanced Nano Characterization, The University of Tokyo, supported by Ministry of Education, Culture, Sports, Science and Technology (MEXT). T.S. acknowledges the financial support of the World Premier International Center Initiative (WPI) on Materials Nanoarchitectonics, MEXT.

Supporting Information Available: XRD pattern of SrTiO₃ thin film fabricated on a glass substrate by NS-LSPE. This material is available free of charge via the Internet at <http://pubs.acs.org>.

REFERENCES AND NOTES

- Yu, L. S.; Harper, J. M. E.; Cuomo, J. J.; Smith, D. A. Alignment of Thin Films by Glancing Angle Ion Bombardment during Deposition. *Appl. Phys. Lett.* **1985**, *47*, 932–933.
- Hasegawa, K.; Fujino, K.; Mukai, H.; Konishi, M.; Hayashi, K.; Sato, K.; Honjo, S.; Sato, Y.; Ishii, H.; Iwata, Y. Biaxially Aligned YBCO Film Tapes Fabricated by All Pulsed Laser Deposition. *Appl. Supercond.* **1998**, *4*, 487–493.
- Shibata, T.; Fukuda, K.; Ebina, Y.; Kogure, T.; Sasaki, T. One-Nanometer-Thick Seed Layer of Unilamellar Nanosheets Promotes Oriented Growth of Oxide Crystal Films. *Adv. Mater.* **2008**, *20*, 231–235.
- Shibata, T.; Ebina, Y.; Ohnishi, T.; Takada, K.; Kogure, T.; Sasaki, T. Fabrication of Anatase Thin Film with Perfect c-Axis Orientation on Glass Substrate Promoted by a Two-Dimensional Perovskite Nanosheet Seed Layer. *Cryst. Growth Des.* **2010**, *10*, 3787–3793.
- Shibata, T.; Ohnishi, T.; Sakaguchi, I.; Osada, M.; Takada, K.; Kogure, T.; Sasaki, T. Well-Controlled Crystal Growth of Zinc Oxide Films on Plastics at Room Temperature Using 2D Nanosheet Seed Layer. *J. Phys. Chem. C* **2009**, *113*, 19096–19101.
- Kikuta, K.; Noda, K.; Okumura, S.; Yamaguchi, T.; Hirano, S. Orientation Control of Perovskite Thin Films on Glass Substrates by the Application of a Seed Layer Prepared from Oxide Nanosheets. *J. Sol–Gel Sci. Technol.* **2007**, *42*, 381–387.

7. Shibata, T.; Takano, H.; Ebina, Y.; Kim, D. S.; Ozawa, T. C.; Akatsuka, K.; Ohnishi, T.; Takada, K.; Kogure, T.; Sasaki, T. Versatile van der Waals Epitaxy-like Growth of Crystal Films Using Two-Dimensional Nanosheets as a Seed Layer: Orientation Tuning of SrTiO_3 Films along Three Important Axes on Glass Substrates. *J. Mater. Chem. C* **2014**, *2*, 441.
8. Ma, R.; Sasaki, T. Nanosheets of Oxides and Hydroxides: Ultimate 2D Charge-Bearing Functional Crystallites. *Adv. Mater.* **2010**, *22*, 5082–5104.
9. Yamada, N.; Shibata, T.; Taira, K.; Hirose, Y.; Nakao, S.; Lam, N.; Hoang, N. L. H.; Hitosugi, T.; Shimada, T.; Sasaki, T.; et al. Enhanced Carrier Transport in Uniaxially (001)-Oriented Anatase $\text{Ti}_{0.94}\text{Nb}_{0.06}\text{O}_2$ Films Grown on Nanosheet Seed Layers. *Appl. Phys. Express* **2011**, *4*, 045801.
10. Jung, C.; Ohnishi, T.; Osada, M.; Takada, K.; Sasaki, T. Oriented Film Growth of $\text{Ba}_{1-x}\text{Sr}_x\text{TiO}_3$ Dielectrics on Glass Substrates Using 2D Nanosheet Seed Layer. *ACS Appl. Mater. Interfaces* **2013**, *5*, 4592–4596.
11. Kondoh, Y.; Sasajima, K.; Hayashi, M.; Kimura, J.; Takuwa, I.; Ehara, Y.; Funakubo, H.; Uchida, H. Crystal Orientation Control of Bismuth Layer-Structured Dielectric Films Using Interface Layers of Perovskite-Type Oxides. *Jpn. J. Appl. Phys.* **2011**, *50*, 09NA04.
12. Hatalis, M.; Greve, D. High-Performance Thin-Film Transistors in Low-Temperature Crystallized LPCVD Amorphous Silicon Films. *IEEE Electron Device Lett.* **1987**, *8*, 361–364.
13. Koida, T.; Kondo, M.; Tsutsumi, K.; Sakaguchi, A.; Suzuki, M.; Fujiwara, H. Hydrogen-Doped In_2O_3 Transparent Conducting Oxide Films Prepared by Solid-Phase Crystallization Method. *J. Appl. Phys.* **2010**, *107*, 033514.
14. Ebata, K.; Tomai, S.; Tsuruma, Y.; Itsuka, T.; Matsuzaki, S.; Yano, K. High-Mobility Thin-Film Transistors with Polycrystalline In–Ga–O Channel Fabricated by DC Magnetron Sputtering. *Appl. Phys. Express* **2012**, *5*, 011102.
15. Hoang, N. L. H.; Hirose, Y.; Nakao, S.; Hasegawa, T. Crystallization Kinetics of Amorphous Sputtered Nb-Doped TiO_2 Thin Films. *Appl. Phys. Express* **2011**, *4*, 105601.
16. Ishiwara, H.; Yamamoto, H.; Furukawa, S.; Tamura, M.; Tokuyama, T. Lateral Solid Phase Epitaxy of Amorphous Si Films on Si Substrates with SiO_2 Patterns. *Appl. Phys. Lett.* **1983**, *43*, 1028–1030.
17. Furubayashi, Y.; Hitosugi, T.; Yamamoto, Y.; Inaba, K.; Kinoda, G.; Hirose, Y.; Shimada, T.; Hasegawa, T. A Transparent Metal: Nb-Doped Anatase TiO_2 . *Appl. Phys. Lett.* **2005**, *86*, 252101.
18. Hirose, Y.; Yamada, N.; Nakao, S.; Hitosugi, T.; Shimada, T.; Hasegawa, T. Large Electron Mass Anisotropy in a d-Electron-Based Transparent Conducting Oxide: Nb-Doped Anatase TiO_2 Epitaxial Films. *Phys. Rev. B* **2009**, *79*, 165108.
19. Hitosugi, T.; Yamada, N.; Nakao, S.; Hatabayashi, K.; Shimada, T.; Hasegawa, T. Structural Study of TiO_2 -Based Transparent Transport Conducting Films. *J. Vac. Sci. Technol., A* **2008**, *26*, 1027–1029.
20. Hitosugi, T.; Ueda, A.; Nakao, S.; Yamada, N.; Furubayashi, Y.; Hirose, Y.; Shimada, T.; Hasegawa, T. Fabrication of Highly Conductive $\text{Ti}_{1-x}\text{Nb}_x\text{O}_2$ Polycrystalline Films on Glass Substrates via Crystallization of Amorphous Phase Grown by Pulsed Laser Deposition. *Appl. Phys. Lett.* **2007**, *90*, 212106.
21. Chen, T. L.; Hirose, Y.; Hitosugi, T.; Hasegawa, T. One Unit-Cell Seed Layer Induced Epitaxial Growth of Heavily Nitrogen Doped Anatase TiO_2 Films. *J. Phys. D: Appl. Phys.* **2008**, *41*, 062005.
22. Okumoto, T. Unpublished.
23. Mitchell, D.; Attard, D.; Triani, G. Transmission Electron Microscopy Studies of Atomic Layer Deposition TiO_2 Films Grown on Silicon. *Thin Solid Films* **2003**, *441*, 85–95.